Published in final edited form as:
J Neurochem. 2006 September ; 98(5): . doi:10.1111/j.1471-4159.2006.04063.x.

Glutamate-induced protease-mediated loss of plasma membrane Ca^{2+} pump activity in rat hippocampal neurons

William J. Pottorf II[*,1], **Tanner M. Johanns**[*], **Stephen M. Derrington**[*], **Emanuel E. Strehler**[†], **Agnes Enyedi**[‡], and **Stanley A. Thayer**[*]

[*]Department of Pharmacology, University of Minnesota Medical School, Minneapolis, Minnesota, USA

[†]Department of Biochemistry and Molecular Biology, Mayo Clinic College of Medicine, Rochester, Minnesota, USA

[‡]National Medical Center, Dioszegi, Budapest, Hungary

Abstract

Ca^{2+} dysregulation is a hallmark of excitotoxicity, a process that underlies multiple neurodegenerative disorders. The plasma membrane Ca^{2+} ATPase (PMCA) plays a major role in clearing Ca^{2+} from the neuronal cytoplasm. Here, we show that the rate of PMCA-mediated Ca^{2+} efflux from rat hippocampal neurons decreased following treatment with an excitotoxic concentration of glutamate. PMCA-mediated Ca^{2+} extrusion following a brief train of action potentials exhibited an exponential decay with a mean time constant (τ) of 8.8 ± 0.2 s. Four hours following the start of a 30 min treatment with 200 μM glutamate, a second population of cells emerged with slowed recovery kinetics (τ = 16.5 ± 0.3 s). Confocal imaging of cells expressing an enhanced green fluorescent protein (EGFP)-PMCA4b fusion protein revealed that glutamate treatment internalized EGFP and that cells with reduced plasma membrane fluorescence had impaired Ca^{2+} clearance. Treatment with inhibitors of the Ca^{2+}-activated protease calpain protected PMCA function and prevented EGFP-PMCA internalization. PMCA internalization was triggered by activation of NMDA receptors and was less pronounced for a non-toxic concentration of glutamate relative to one that produces excitotoxicity. PMCA isoform 2 also internalized following exposure to glutamate, although the Na^+/K^+ ATPase did not. These data suggest that glutamate exposure initiated protease-mediated internalization of PMCAs with a corresponding loss of function that may contribute to the Ca^{2+} dysregulation that accompanies excitotoxicity.

Keywords

calpain; caspase; excitotoxicity; glutamate; plasma membrane calcium ATPase; plasma membrane calcium pump

Efficient removal of Ca^{2+} from the cytoplasm is essential for maintaining the spatial and temporal fidelity of Ca^{2+} signals and is required to prevent Ca^{2+} from accumulating to toxic levels. The plasma membrane Ca^{2+} ATPase (PMCA) is an integral part of the Ca^{2+} regulatory system in neurons (Thayer *et al*. 2002). These Ca^{2+} pumps utilize the energy from ATP hydrolysis for the uphill translocation of Ca^{2+} across the plasmalemma (Carafoli

Address correspondence and reprint requests to S. A. Thayer, Department of Pharmacology, University of Minnesota Medical School, 6–120 Jackson Hall, 321 Church St. S.E., Minneapolis, MN 55455, USA. sathayer@umn.edu.
[1]The present address of William J. Pottorf II is AstraZeneca LP, 1800 Concord Pike, Wilmington, DE 19850, USA.

and Brini 2000). PMCAs play a prominent role in maintaining a low resting intracellular Ca^{2+} concentration ($[Ca^{2+}]_i$) in neurons, and in returning $[Ca^{2+}]_i$ to basal levels following moderate stimuli of the order of 1–10 action potentials (Benham *et al*. 1992; Werth *et al*. 1996). PMCA-mediated Ca^{2+} clearance has been shown to control neurotransmitter release (Zenisek and Matthews 2000), excitability (Usachev *et al*. 2002) and gene expression (Husain *et al*. 1997). Reduced PMCA expression puts neuronal cells at risk for Ca^{2+}-induced toxicity (Garcia *et al*. 2001), and oxidative stress results in PMCA inactivation (Zaidi *et al*. 2003).

The C-termini of PMCAs bind calmodulin, which stimulates the enzyme by relief of autoinhibition. Thus, transient increases in $[Ca^{2+}]_i$ will reversibly stimulate PMCA-mediated Ca^{2+} clearance through a calmodulin-dependent process (Caride *et al*. 2001; Pottorf and Thayer 2002). Autoinhibition can also be relieved by proteolysis of the PMCA by the Ca^{2+}-activated protease, calpain, that cleaves the C-terminal region within the calmodulin-binding domain (James *et al*. 1989). Thus, calpain will irreversibly stimulate PMCA4-mediated Ca^{2+} pumping activity by relieving autoinhibition. Similarly, caspase 3 will cleave the C-terminus of PMCA4b, resulting in increased Ca^{2+} pumping activity (Paszty *et al*. 2002, 2005).

Schwab *et al*. (2002) have also shown that activation of the apoptotic cascade, specifically caspases 1 and 3, cleaved PMCA isoforms 2 and 4. They found that caspase-mediated cleavage inactivated the PMCA, and that mutation of the caspase cleavage site protected cells from a rapid form of cell death (Schwab *et al*. 2002). It is not clear whether large increases in neuronal $[Ca^{2+}]_i$ induce activation or degradation of the PMCA.

Here, we show that exposure to toxic concentrations of glutamate leads to protease-mediated internalization of the PMCA and a corresponding loss of PMCA function. We suggest that loss of PMCA function may contribute to the Ca^{2+} dysregulation that accompanies excitotoxicity, and that protecting the PMCA from protease-mediated endocytosis may enhance neuronal survival following toxic insult.

Materials and methods

Materials

Dulbecco's modified Eagle's medium (DMEM), fetal bovine serum and horse serum were purchased from Gibco-BRL (Grand Island, NY, USA). Indo-1 AM, X-rhod AM and pluronic F-127 were obtained from Molecular Probes (Eugene, OR, USA). All other reagents were purchased from Sigma (St. Louis, MO, USA).

Cell culture

Rat hippocampal neurons were grown in primary culture as described previously (Wang *et al*. 1994) with minor modifications. Fetuses were removed on embryonic day 17 from maternal rats, anesthetized with CO_2 and killed by decapitation under a protocol approved by the University of Minnesota Institutional Animal Care and Use Committee in accordance with the National Institutes of Health guide for the care and use of laboratory animals. Hippocampi were dissected and placed in Ca^{2+}- and Mg^{2+}-free HEPES-buffered Hank's salt solution (HHSS), pH 7.45. HHSS was composed of the following (in mM): HEPES 20, NaCl 137, $CaCl_2$ 1.3, $MgSO_4$ 0.4, $MgCl_2$ 0.5, KCl 5.0, KH_2PO_4 0.4, Na_2HPO_4 0.6, $NaHCO_3$ 3.0 and glucose 5.6. Cells were dissociated by trituration through a 5 mL pipette and a series of flame-narrowed Pasteur pipettes. Cells were pelleted, then re-suspended in DMEM without glutamine, supplemented with 10% fetal bovine serum and penicillin/streptomycin (100 U/mL and 100 μg/mL, respectively). Dissociated cells then were plated at a density of 10 000–15 000 cells/well onto 25 mm round cover glasses that had been coated

with poly D-lysine (0.1 mg/mL) and washed with H_2O. Neurons were grown in a humidified atmosphere of 10% CO_2 and 90% air (pH 7.4) at 37°C, and fed at days 1 and 6 by exchange of 75% of the medium with DMEM supplemented with 10% horse serum and penicillin/streptomycin. Cells used in these experiments were cultured without mitotic inhibitors for a minimum of 10 days and a maximum of 15 days.

Expression of EGFP-PMCA fusion proteins

Expression vectors encoding PMCA4b, PMCA2xb and PMCA2wb fused at their NH_2 termini to EGFP (EGFP-PMCA4b, EGFP-PMCA2xb and EGFP-PMCA2wb) were constructed by cloning the specified PMCA sequence into pEGFP-C1 (Clontech, Palo Alto, CA, USA) as previously described (Chicka and Strehler 2003). All expression vectors used in this study contained the cytomegalovirus promoter.

Hippocampal neurons were transfected with plasmid DNA using the calcium phosphate procedure described by Xia *et al*. (1996), with some modifications. Briefly, 10–14 days after plating, hippocampal neurons were transferred into serum-free DMEM (2 mL/well, six-well plate) supplemented with 1 mM sodium kyneurate, 10 mM $MgCl_2$ and 5 mM HEPES, pH 7.5, for 15 min. The conditioned medium was saved. A DNA/calcium phosphate precipitate for one six-well plate was prepared by mixing 500 μL 250 mM $CaCl_2$ and 15 μL plasmid DNA (about 1 μg/μL) with an equal volume of 2× HEPES-buffered salt solution (274 mM NaCl, 10 mM KCl, 1.4 mM Na_2HPO4, 15 mM D-glucose, 42 mM HEPES, pH 7.07). The precipitate was allowed to form for 25–30 min at room temperature (22°C, RT) before addition to the cultures. A 60 μL volume of the DNA/calcium phosphate precipitate was added drop-wise to each well. Plates were then returned to the 10% CO_2 incubator. After 20–25 min, the incubation was stopped by washing cells three times with 3 mL/well DMEM. The saved conditioned medium was put back in each well and the cells were returned to a 10% CO_2 incubator at 37°C. The transfection efficiency ranged from 2 to 11%.

Microfluorimetry

$[Ca^{2+}]_i$ was determined using a previously described dual-emission microfluorimeter (Werth and Thayer 1994) to monitor the Ca^{2+}-sensitive fluorescent chelator, indo-1 (Grynkiewicz *et al*. 1985). Cells were incubated with indo-1 AM (5 μM) and pluronic F-127 (0.02% w/v) in HHSS at RT for 25 min, washed with HHSS for 10 min and then incubated for 15 min in HHSS containing 5 μM cyclopiazonic acid (CPA) and 10 μM 6-cyano-7-nitroquinoxaline-2,3,-dione (CNQX). Loaded, washed cells were mounted in a flow-through chamber equipped with platinum electrodes (Thayer *et al*. 1988). The chamber was mounted on an inverted epifluorescence microscope (Diaphot, Nikon, Melville, NY, USA) and cells were localized by phase-contrast illumination with a 70× objective. Action potentials were evoked by electric field stimulation as described previously (Piser *et al*. 1994).

Indo-1 was excited at 350 (10) nm and emission detected at 405 (20) nm and 490 (20) nm. Changes in indo-1 fluorescence were converted to $[Ca^{2+}]_i$ by using the formula $[Ca^{2+}]_i = K_d\beta(R-R_{min})/(R_{max}-R)$, where R is the 405/490 nm fluorescent intensity ratio. The dissociation constant (K_d) used for Indo-1 was 250 nM, and β was the ratio of emitted fluorescence at 490 nm in the absence and presence of calcium. R_{min}, R_{max} and β were determined in ionomycin-permeabilized cells in calcium-free (1 mM EGTA) and 5 mM Ca^{2+} buffers. Values of R_{min}, R_{max} and β were 1.28, 14.11 and 3.63, respectively.

Confocal microscopy

After 24–48 h, transfected neurons were removed from the growth medium and transferred to a chamber containing HHSS. Neurons were imaged with a Fluoview 300 laser scanning confocal microscope attached to an inverted Olympus IX70 microscope equipped with a

PlanApo 60× objective (NA 1.40) (Olympus Optical, Tokyo, Japan). Optimal images were obtained by averaging four scans using Kalman filtering. The excitation and emission wavelengths for EGFP and FITC were 488 nm and 522 (16) nm, respectively. The excitation and emission wavelengths for tetramethyl rhodamine isothiocyanate (TRITC) were 540 nm and > 605 nm, respectively. $[Ca^{2+}]_i$ was measured in EGFP-PMCA-expressing cells using the Ca^{2+} indicator, X-rhod, which was excited at 540 nm and detected at > 605 nm. Cells were loaded with the indicator by incubating in 2 μM X-rhod AM for 45 min at RT. After washing for 10 min, $[Ca^{2+}]_i$ increases evoked by electric field stimulation were imaged in a non-nuclear region of interest within the soma.

Immunocytochemistry

For labeling endogenous PMCAs, cells were washed with phosphate-buffered saline (PBS) without Ca^{2+} and Mg^{2+} (PBS-CM, 0.1 M, 7.4 pH) and fixed with 4% paraformaldehyde and 4% sucrose for 15 min at RT. Following washing with PBS-CM (3 × 5 min), cells were further fixed and permeabilized in ice-cold methanol for 15 min at − 20°C. After extensive washing with PBS-CM, cells were blocked with 5% rabbit serum + 1% bovine serum albumin (BSA) for 1 h, then incubated for 1 h at RT with monoclonal pan-anti-PMCA antibody 5F10 (1: 2000 in 10% rabbit serum). After washing in PBS + CM (3 × 5 min), cells were incubated for 1 h at RT in darkness with secondary anti-mouse FITC antibody (1: 400 in 2% BSA; DakoCytomation California Inc., Carpinteria, CA, USA) and washed in PBS + CM (3 × 5 min). Fixed cells were mounted on slides with Fluoromount-G (SouthernBiotech, Birmingham, AL, USA) and air dried. Immunofluorescence was observed using confocal microscopy.

For labeling the Na^+, K^+ ATPase and human PMCA4b, cells were washed with PBS-CM, fixed with 4% paraformaldehyde for 30 min at RT and washed with PBS-CM (3 × 5 min). After a 30 min pre-incubation in 1% rabbit serum and 0.1% Triton, cells were incubated in primary antibody [anti-Na, K ATPase α5 at 1: 400 (Developmental Studies Hybridoma Bank, Iowa City, IA, USA) or anti-human PMCA4b (JA3, Affinity BioReagents, Golden, CO, USA) at 1: 400], placed in a humid chamber and incubated for 36–48 h at 4°C. Cells were then washed with 1% rabbit serum and incubated in secondary anti-mouse TRITC antibody (1: 200 for Na, K ATPase; 1: 400 for hPMCA4b; DakoCytomation California Inc.) for 30 min at RT and washed with PBS-CM (3 × 5 min). Fixed cells were mounted on slides with Fluoromount-G and air dried. Immunofluorescence was observed using confocal microscopy.

Statistical analysis

Data presented in results are expressed as mean ± SEM; *n*, number of cells tested. Statistical significance was determined by either two-way ANOVA with Fisher's PLSD-posthoc test or by Student's *t*-test where indicated. Statistical significance of image scores was determined by the χ^2 test. A $p < 0.05$ was accepted as the level of significance. Mono-exponential decay functions were fitted to the data using a non-linear, least-squares curve fitting algorithm (correlation coefficient > 0.97) and histograms were fitted to a Gaussian model (correlation coefficient > 0.87) using ORIGIN 6.1 software.

Results

Glutamate-induced inhibition of Ca^{2+} clearance

The clearance of small (< 400 nM) increases in $[Ca^{2+}]_i$ from the neuronal cytoplasm is primarily accomplished by ATP-ases that pump Ca^{2+} across the plasmalemma and into the endoplasmic reticulum. We evoked brief trains of action potentials in indo-1 AM-loaded hippocampal neurons by electric field stimulation (4 s, 8 Hz) to elicit a rapid increase in

$[Ca^{2+}]_i$. In the presence of CPA (5 μM) to block the sarcoplasmic and endoplasmic reticulum Ca^{2+} ATPase (SERCA), the $[Ca^{2+}]_i$ recovered by a process well fit by a mono-exponential equation, with a mean time constant (τ) of 8.8 ± 0.2 s (*n* = 120) (Figs 1a and b). Immunocytochemistry with pan-anti-PMCA antibody 5F10 revealed PMCA immunoreactivity primarily localized to the plasma membrane (Fig. 1b inset). Thus, under control conditions, PMCA is primarily localized to the plasma membrane, consistent with previous reports (Kip *et al*. 2006).

Recovery from the small action potential-induced increases in $[Ca^{2+}]_i$ shown in Fig. 1(a) was predominantly mediated by the PMCA. Mitochondrial Ca^{2+} uptake had a relatively minor influence on the $[Ca^{2+}]_i$ recovery kinetics studied under these recording conditions. The mean time constant recorded from cells treated with 2.5 μM antimycin A1 for 30 min increased by only 14 ± 4% and was not significantly different from matched controls (*n* = 14). Small changes in the Na^+ gradient have large effects on the Na^+/Ca^{2+} exchanger due to the $3Na^+$: Ca^{2+} exchange ratio (Hilgemann 2004). Reducing extracellular Na^+ from 144 to 72 mM (substituted reciprocally with *N*-methyl-D-glucamine) did not significantly affect recovery kinetics relative to matched controls (*n* = 13). This reduction in extracellular Na^+ would be predicted to produce a hyperpolarizing shift in the reversal potential for $3Na^+/Ca^{2+}$ exchange, such that the exchanger, if active, would operate in the reverse mode at resting membrane potential. However, τ for $[Ca^{2+}]_i$ recovery was increased by only 16 ± 4% under these conditions, suggesting a minor role for Na^+/Ca^{2+} exchange in returning $[Ca^{2+}]_i$ to basal levels following brief trains of action potentials. The PMCA exchanges 2 H^+ for each Ca^{2+} and thus, is inhibited by alkaline extracellular pH (Benham *et al*. 1992; Schwiening *et al*. 1993). Increasing the extracellular pH to 9.0 significantly increased τ to 202 ± 18% of control (*n* = 6; $p < 0.01$, Student's paired *t*-test), indicating that the PMCA is the predominant mechanism of recovery from action potential-induced increases in $[Ca^{2+}]_i$ under these recording conditions.

We next examined hippocampal neurons 4 h after a 30 min exposure to the excitotoxin, glutamate (200 μM), using recovery kinetics from field stimulation-induced $[Ca^{2+}]_i$ increases as an index of PMCA function. The mean τ increased significantly to 11.5 ± 0.4 s (*n* = 138; $p < 0.001$) (Figs 1c and d). The increase appeared to result from the emergence of a new population of cells with slowed recovery kinetics. As shown in Fig. 1(d), the frequency histogram for the recovery time constant could be optimally fit by two Gaussian curves describing a population of cells with control recovery kinetics (τ = 8.7 ± 0.3 s) and a new population with slowed recovery (τ = 16.5 ± 0.4 s). This observation is consistent with the stochastic nature of glutamate-induced neurotoxicity, in that even though virtually every cell responds to this concentration of glutamate (Randall and Thayer 1992), individual cells will display an independent time course for cell death (Dubinsky *et al*. 1995). Interestingly, we also noted that a number of cells displayed internalized PMCA immunoreactivity following treatment with glutamate. PMCA immunoreactivity at the plasma membrane appeared to decrease, and labeling appeared in the cytoplasm possibly within vesicular structures (Fig. 1d inset).

We next determined whether internalized PMCA predicted slowed recovery kinetics. Twenty-four hours after transfection of the hippocampal culture with a plasmid encoding EGFP fused to PMCA4b, confocal imaging revealed green fluorescence primarily localized to the plasma membrane (Fig. 2a, left panel). Thus, PMCA4b with EGFP fused to the amino terminus (EGFP-PMCA4b) targets appropriately to the plasma membrane. In these images, the confocal z plane in which the plasma membrane could most clearly be resolved from the cytoplasm is shown in order to detect internalization. The cells extended EGFP-PMCA-labeled processes that lie in a plane just above the surface of the coverslip and well below the largest cross-section of the soma. In this set of experiments, neurons were transfected

with the EGFP-PMCA4b expression vector and, 24 h later, loaded with the $[Ca^{2+}]_i$ indicator X-rhod AM. Four hours following treatment with 200 μM glutamate, confocal images of EGFP localization were collected and the cells scored according to the ranking shown in Fig. 2(a). A score of 1 indicated fluorescence exclusively localized to the plasma-lemma; a score of 2 indicated strong plasmalemma labeling with some internal labeling; a score of 3 indicated weak plasmalemma labeling and strong intracellular labeling; and a cell was scored 4 if plasmalemmal labeling was minimal and internal labeling strong. Scoring preceded measuring recovery kinetics, so the investigator was blinded to the yet to be determined τ. Similar to the results from indo-1-based $[Ca^{2+}]_i$ measurements, the mean τ for recovery measured with X-rhod-based confocal microscopy increased by 29% following treatment with glutamate. Representative $[Ca^{2+}]_i$ recordings are shown in Fig. 2(b), illustrating that increasing score predicted slowed recovery kinetics. Indeed, recovery kinetics displayed a graded slowing with increased score (Fig. 2c). Thus, loss of plasmalemmal PMCA predicts impaired Ca^{2+} regulation.

PMCA selectively internalizes

We next confirmed that the EGFP remained attached to the full-length hPMCA4b protein in the live cell imaging experiments. Antibody JA3 is species-specific and thus, only recognizes a C-terminal epitope of exogenously expressed human PMCA4 in rat hippocampal cultures (Caride *et al*. 1996). We fixed EGFP-hPMCA4b-expressing cells, after either sham treatment or treatment with glutamate, and performed immunocytochemistry to label hPMCA4. As shown in Fig. 3(a), EGFP fluorescence (green) and hPMCA4 immunoreactivity (red) completely overlapped (yellow) in the merged images.

We also explored the possibility that glutamate was causing generalized internalization of membrane proteins. Thus, we fixed EGFP-PMCA4b-expressing cells after either sham treatment or treatment with glutamate and performed immunocytochemistry to label the Na^+/K^+ ATPase. As shown in Fig. 3(b), PMCA4 and the Na^+/K^+ ATPase were both localized to the plasma membrane in untreated hippocampal neurons. However, 4 h after the start of a 30 min treatment with 200 μM glutamate, EGFP-PMCA4b was significantly internalized, in contrast to the Na^+/K^+ ATPase, which remained on the plasma membrane. Using the scoring system described in Fig. 2 (1 = plasma membrane localized; 4 = internalized), an investigator uninformed of the fluorophore scored glutamate-treated EGFP fluorescence significantly higher than the co-labeled Na^+/K^+ ATPase; 39% of the EGFP images were scored 3 or greater, whereas only 10% of the Na^+/K^+ ATPase immunoreactivity received comparable scores ($p < 0.05$, $n = 34$, χ^2). In untreated cells, 100% of the EGFP-PMCA4b and Na^+/K^+ ATPase immunoreactivity images were scored as 2 or less.

PMCA internalizes following activation of NMDA receptors

We next determined the type of glutamate receptor mediating internalization of the PMCA. Using the scoring system described in Fig. 2 (1 = plasma membrane localized; 4 = internalized), an investigator uninformed of the treatment scored images of glutamate-treated EGFP-PMCA-expressing cells significantly higher than untreated cells (Fig. 4a). In control experiments, 91% ($n = 130$) of the cells were scored 2 or less. Following treatment with glutamate, 57% ($n = 124$) of the cells were scored 3 or 4, a significant increase relative to control ($p < 0.0001$ χ^2), indicating that the excitotoxin induced the internalization of EGFP-PMCA fluorescence. Treatment with 20 μM glutamate increased the fraction of cells scoring 3 or 4 significantly above control values ($p < 0.05$, χ^2) (Fig. 4b), even though this concentration is not itself toxic (Choi *et al*. 1987). The internalization appeared to be concentration-dependent, because treatment with 20 μM glutamate resulted in only 35% ($n = 31$) of the cells being scored 3 or 4. We hypothesized that this dramatic change in Ca^{2+}

pump distribution was triggered by activation of NMDA receptors. Consistent with this prediction, treatment with the selective agonist, NMDA (200 μM; 30 min), induced levels of internalization comparable with those produced by glutamate (Fig. 4b).

Protease inhibitors protect PMCA from functional loss following glutamate treatment

We next examined the mechanism of the loss of functional Ca^{2+} clearance. Schwab *et al*. (2002) have shown that activation of caspases will degrade certain PMCA isoforms. We tested the hypothesis that glutamate-induced activation of proteases produced a loss of PMCA function. Prior to exposure to glutamate, we treated the cells for 60 min with calpeptin, an inhibitor of the Ca^{2+}-activated protease calpain, and Z-VAD-fmk, a pan-caspase inhibitor (Fig. 5). Glutamate treatment failed to impair Ca^{2+} clearance in cells pre-treated with calpeptin (10 μM) and Z-VAD-fmk (100 μM). The protease inhibitors in combination protected the hippocampal neurons from glutamate-induced loss of PMCA function (Fig. 5a). The mean τ for recovery in these cells was 8.2 ± 0.2 s (n = 51), a value comparable with the control (Fig. 1a). We also examined the effects of each inhibitor on $[Ca^{2+}]_i$ recovery kinetics individually. Calpeptin alone also protected cells from glutamate-induced loss of PMCA function (Figs 5c and d). The mean τ for recovery in these cells was 8.4 ± 0.1 s (n = 31). The effects of Z-VAD-fmk were less clear. The mean τ from Z-VAD-fmk-treated cells was 9.7 ± 0.4 s (n = 33), which was not significantly different from control (p = 0.12, ANOVA with Fisher's PLSD posthoc), although the frequency histogram (Fig. 5f) suggested the emergence of a set of cells with slowed recovery kinetics. The mean τ from Z-VAD-fmk-treated cells was significantly slower than that for cells treated with calpeptin and Z-VAD-fmk in combination ($p < 0.05$).

Protease inhibitors also prevented glutamate-induced internalization of EGFP-PMCA4b. Using the scoring system described in Fig. 2 (1 = plasma membrane localized; 4 = internalized), an investigator uninformed of the treatment scored images of glutamate-treated cells significantly higher than untreated cells (Fig. 6). In control experiments, 91% (n = 130) of the cells were scored 2 or less and following treatment with glutamate, 57% (n = 124) of the cells were scored 3 or 4. Seventy-six percent (n = 60) of cells incubated with calpeptin and Z-VAD-fmk prior to, and during treatment with glutamate were scored 2 or less, which is similar to control cells. Calpeptin (10 μM) alone also prevented PMCA internalization, as did another calpain inhibitor, MDL 28170 (10 μM). Seventy-eight percent (n = 32) of the calpeptin-treated cells and 82% (n = 17) of the MDL28170-treated cells were scored 2 or less, which is significantly different from cells treated with glutamate alone ($p < 0.001$, calpeptin + glutamate vs. glutamate; $p < 0.01$, MDL28170 + glutamate vs. glutamate; χ^2). Calpeptin (10 μM) did not affect the increase in $[Ca^{2+}]_i$ evoked by glutamate (200 μM, 2 min), as indicated by photometry with the low affinity Ca^{2+} indicator, indo-5F (p = 0.48; n = 6). Taken together, the results indicate that treatment with glutamate causes a calpain-mediated loss of PMCA from the plasmalemma, and those cells with less Ca^{2+} pump in the plasma membrane have slowed recovery kinetics.

Glutamate-induced internalization of PMCA isoforms 2 and 4

Calpain cleaves PMCA4b and PMCA2 at different sites (Guerini *et al*. 2003). To determine whether the site of cleavage by calpain was important for glutamate-induced internalization of PMCA, we studied additional PMCA isoforms. EGFP-PMCA2xb and EGFP-PMCA2wb localized to the plasma membrane of untreated hippocampal neurons in a similar way to EGFP-PMCA4b (Fig. 7). Following exposure to glutamate, green fluorescence internalized in cells expressing EGFP-PMCA4b, EGFP-PMCA2xb and EGFP-PMCA2wb. Using the scoring system described in Fig. 2 (1 = plasma membrane localized; 4 = internalized), an investigator uninformed as to the previous treatment scored glutamate-treated cells significantly higher than untreated cells. Eighty-six percent of control cells expressing

EGFP-PMCA4b scored 2 or less whereas after glutamate exposure, 69% of the cells were scored 3 or greater ($p < 0.0001$, $n = 182$, χ^2). In control cells expressing EGFP-PMCA2wb, 92% of the cells scored 2 or less whereas after glutamate exposure 75% of the cells were scored 3 or greater ($p < 0.0001$, $n = 68$, χ^2). Seventy-four percent of control cells expressing EGFP-PMCA2xb were scored 2 or less whereas after glutamate exposure, 73% of the cells were scored 3 or greater ($p < 0.001$, $n = 60$, χ^2). Thus, glutamate induces the internalization of both PMCA isoforms 2 and 4.

Discussion

Loss of cell-surface EGFP-PMCA from rat hippocampal neurons exposed to glutamate for 30 min correlated with a slowing of Ca^{2+} efflux kinetics. PMCA internalization was triggered by activation of NMDA receptors and was less pronounced for a non-toxic concentration (20 μM) of glutamate relative to one (200 μM) that produces excitotoxicity. PMCA isoforms 2 and 4 were both internalized following glutamate treatment although the Na^+/K^+ ATPase was not, suggesting that the internalization did not result from a global loss of proteins from the plasma membrane. EGFP-PMCA internalization and loss of functional Ca^{2+} clearance were prevented by pre-treatment with the calpain inhibitors, calpeptin and MDL 28170. Because both PMCA internalization and loss of function were initiated by the same stimuli and prevented by protease inhibitors, it is plausible that slowed Ca^{2+} clearance resulted from loss of cell-surface PMCA.

In a previous study we showed that transient (5–15 min) elevation of $[Ca^{2+}]_i$ in sensory neurons resulted in a long-lived (1 h) and reversible acceleration of PMCA-mediated Ca^{2+} efflux (Pottorf and Thayer 2002). We anticipated that large glutamate-induced Ca^{2+} loads would activate calpain, leading to cleavage of the EGFP-PMCA carboxy-terminal regulatory domain and permanent activation of the Ca^{2+} pump, as has been shown *in vitro* (James *et al*. 1989; Paszty *et al*. 2005). This hypothesis was disproved; calpain activation induced down-regulation (likely by internalization) of the PMCA and a slowing of Ca^{2+} efflux kinetics. Schwab *et al*. (2002) described caspase-mediated cleavage and internalization of PMCA4 during staurosporine-induced apoptosis. Our results are similar in that glutamate activation of calpain led to the loss of functional PMCA, but we did not detect a significant role for caspases in this process. Glutamate-induced excitotoxicity activates both necrotic and apoptotic pathways (Ankarcrona *et al*. 1995); the predominance of one pathway over the other is sensitive to the model system, and to the intensity and duration of the excitotoxic stimulus (Bonfoco *et al*. 1995; Martin *et al*. 1998). Calpain-mediated PMCA internalization is the predominant action observed 4 h after treating hippocampal neurons with glutamate, although other pathways may be recruited later.

Calpain-triggered loss of PMCA-mediated Ca^{2+} clearance may have resulted from PMCA degradation, endocytosis or, possibly, internalization followed by transport to the lysosome. Indeed, while both PMCA4 and PMCA2 are calpain substrates, it is not clear whether glutamate-induced internalization resulted from a direct cleavage of the PMCA, or whether calpain acted upstream of the Ca^{2+} pump (e.g. on a cytoskeletal component involved in membrane retrieval) to trigger the internalization process. In some images, internalized EGFP-PMCA4 appeared to reside within vesicular structures (e.g. Figure 7). Calpains may be involved in the formation of coated vesicles and vesicle fusion to endosomes (Sato *et al*. 1995). Whether the PMCA can recycle to the plasma membrane is not known, although this possibility suggests a novel mechanism by which cells could regulate cell-surface PMCA levels.

The possibility that PMCA internalization occurs during physiological signaling was supported by the observation that a non-toxic concentration of glutamate (20 μM) induced a

small but significant internalization. Clearly, all of the cells studied were healthy at the time of recording or imaging, as indicated by low resting $[Ca^{2+}]_i$ or a visually intact plasma membrane, respectively. However, over 75% of the cells treated with 200 μM glutamate were destined to die (Choi *et al*. 1987). It is plausible that loss of PMCA function is an early event that contributes to the $[Ca^{2+}]_i$ dysregulation, which is thought to underlie excitotoxic death. PMCA internalization may also play a physiological role, regulating Ca^{2+} homeostasis, and contribute to excitotoxicity only after excessive, prolonged activation of NMDA receptors. Aberrant activation of physiological processes that regulate synaptic plasticity, metabolism and gene expression contribute to Ca^{2+}-dependent excitotoxicity (Sattler and Tymianski 2001; Gilman and Mattson 2002; Nicholls 2004).

Excitotoxin-induced increases in Ca^{2+} initiate calpain-mediated degradation of NMDA receptors (Wu *et al*. 2005) presumably as part of a mechanism to protect from over-stimulation. Why would the cell internalize Ca^{2+} clearance proteins such as the PMCAs following exposure to excitotoxin? Without ATP-driven Ca^{2+} efflux the cell would be more vulnerable to stresses that result in elevated Ca^{2+}, such as high frequency stimulation or impaired metabolism. Indeed, loss of Ca^{2+} clearance processes might contribute to the Ca^{2+} dysregulation that follows excitotoxic stimuli (Randall and Thayer 1992; Tymianski *et al*. 1993). One possibility is that calpain initially cleaves the PMCA while it is still embedded in the plasma membrane. This would activate the pump, thereby helping the cell to stem the excess Ca^{2+} influx during the early phase of excitotoxicity. This might suffice to protect the cell from Ca^{2+} overload and death if the insult were mild and of short duration. Eventually, however, the constitutively-activated pumps would need to be turned off, which would conveniently occur by internalization and degradation. This process itself may also be triggered by calpain. Under conditions of long-lasting excitotoxic stimulation, the continuous calpain-mediated loss of PMCA from the membrane might deplete the PMCA pool at the plasma membrane, leading to impaired Ca^{2+} efflux and hastening the demise of the cell. On the other hand, Connor and colleagues observed a reduction in voltage-gated Ca^{2+} channels and a depletion of intracellular Ca^{2+} stores following the initial elevation in $[Ca^{2+}]_i$ evoked by excitotoxin; they hypothesized that Ca^{2+} depletion contributes to excitotoxic death (Connor *et al*. 1999; Xing *et al*. 2004). Indeed, the Ca^{2+} deficiency that results from blocked ionotropic glutamate receptors initiated caspase-mediated cell death in cortical neurons (Yoon *et al*. 2003). This scenario would suggest that cells might reduce Ca^{2+} efflux mechanisms as a means of elevating $[Ca^{2+}]_i$ subsequent to an excessive reduction in Ca^{2+} influx pathways during over-stimulation by glutamate. Glutamate exposure also produces a proteolytic inactivation of the Na^+/Ca^{2+} exchanger, suggesting that down-regulation of Ca^{2+} clearance mechanisms may occur in a co-ordinated manner during excitotoxicity (Bano *et al*. 2005). Loss of PMCA function may represent a form of cross-talk between the apoptotic and necrotic cell death pathways, as suggested by Schwab *et al*. (2002). Thus, inactivation of Ca^{2+} clearance processes may indicate a commitment to cell death.

In summary, we have shown that glutamate induces a calpain-mediated internalization and inactivation of the PMCA in hippocampal neurons. Whether this regulation of pump activity provides a physiological mechanism to fine tune $[Ca^{2+}]_i$ homeostasis, or primarily occurs prior to Ca^{2+}-induced cell death, is not known. Calpain inhibitors show some promise for limiting toxicity during neurodegenerative processes, suggesting that protecting the Ca^{2+} efflux machinery may promote cell survival.

Acknowledgments

We thank Wenna Lin for the preparation of neuronal cultures and Garret Anderson for performing the pH experiments. We thank Aida Filoteo and John Penniston for the generous gift of the PMCA-specific antibodies. The

National Institutes of Health (DA07304, DA11806 to SAT, GM28835 to EES) the National Science Foundation (IBN0110409 to SAT) and the Hungarian Academy of Sciences (OTKA T049476 to AE) supported this work.

Abbreviations used

$[Ca^{2+}]_i$	intracellular calcium concentration
CNQX	6-cyano-7-nitroquinoxaline-2,3-dione
CPA	cyclopiazonic acid
DMEM	Dulbecco's modified Eagle's medium
EGFP	enhanced green fluorescent protein
HHSS	HEPES-buffered Hanks' salt solution
PBS-CM	phosphate-buffered saline without Ca^{2+} and Mg^{2+}
PMCA	plasma membrane Ca^{2+} ATPase
RT	room temperature (22°C)
SERCA	sarcoplasmic and endoplasmic reticulum Ca^{2+} ATPase
TRITC	tetramethyl rhodamin isothiocyante

References

Ankarcrona M, Dypbukt JM, Bonfoco E, Zhivotovsky B, Orrenius S, Lipton SA, Nicotera P. Glutamate-induced neuronal death: a succession of necrosis or apoptosis depending on mitochondrial function. Neuron. 1995; 15:961–973. [PubMed: 7576644]

Bano D, Young KW, Guerin CJ, Lefeuvre R, Rothwell NJ, Naldini L, Rizzuto R, Carafoli E, Nicotera P. Cleavage of the plasma membrane Na+/Ca2+ exchanger in excitotoxicity. Cell. 2005; 120:275–285. [PubMed: 15680332]

Benham CD, Evans ML, McBain CJ. Ca^{2+} efflux mechanisms following depolarization evoked calcium transients in cultured rat sensory neurones. J Physiol. 1992; 455:567–583. [PubMed: 1484362]

Bonfoco E, Krainc D, Ankarcrona M, Nicotera P, Lipton SA. Apoptosis and necrosis — two distinct events induced, respectively, by mild and intense insults with n-methyl-d-aspartate or nitric oxide superoxide in cortical cell cultures. Proc Natl Acad Sci USA. 1995; 92:7162–7166. [PubMed: 7638161]

Carafoli E, Brini M. Calcium pumps: structural basis for and mechanism of calcium transmembrane transport. Curr Opin Chem Biol. 2000; 4:152–161. [PubMed: 10742184]

Caride AJ, Filoteo AG, Enyedi A, Verma AK, Penniston JT. Detection of isoform 4 of the plasma membrane calcium pump in human tissues by using isoform-specific monoclonal antibodies. Biochem J. 1996; 316:353–359. [PubMed: 8645230]

Caride AJ, Penheiter AR, Filoteo AG, Bajzer Z, Enyedi A, Penniston JT. The plasma membrane calcium pump displays memory of past calcium spikes. Differences between isoforms 2b and 4b. J Biol Chem. 2001; 276:39 797–39 804.

Chicka MC, Strehler EE. Alternative splicing of the first intracellular loop of plasma membrane Ca2+-ATPase isoform 2 alters its membrane targeting. J Biol Chem. 2003; 278:18 464–18 470. [PubMed: 12381724]

Choi DW, Maulucci-Gedde M, Kriegstein AR. Glutamate neurotoxicity in cortical cell culture. J Neurosci. 1987; 7:357–368. [PubMed: 2880937]

Connor JA, Razani-Boroujerdi S, Greenwood AC, Cormier RJ, Petrozzino JJ, Lin RCS. Reduced voltage-dependent Ca^{2+} signaling in CA1 neurons after brief ischemia in gerbils. J Neurophysiol. 1999; 81:299–306. [PubMed: 9914290]

Dubinsky JM, Kristal BS, Elizondofournier M. On the probabilistic nature of excitotoxic neuronal death in hippocampal neurons. Neuropharmacology. 1995; 34:701–711. [PubMed: 8532137]

Garcia ML, Usachev YM, Thayer SA, Strehler EE, Winde-bank AJ. Plasma membrane calcium ATPase plays a role in reducing Ca(2+)-mediated cytotoxicity in PC12 cells. J Neurosci Res. 2001; 64:661–669. [PubMed: 11398191]

Gilman CP, Mattson MP. Do apoptotic mechanisms regulate synaptic plasticity and growth-cone motility? Neuromol Med. 2002; 2:197–214.

Grynkiewicz G, Poenie M, Tsien RY. A new generation of Ca^{2+} indicators with greatly improved fluorescence properties. J Biol Chem. 1985; 260:3440–3450. [PubMed: 3838314]

Guerini D, Pan B, Carafoli E. Expression, purification, and characterization of isoform 1 of the plasma membrane Ca2+ pump: focus on calpain sensitivity. J Biol Chem. 2003; 278:38 141–38 148.

Hilgemann DW. New insights into the molecular and cellular workings of the cardiac Na^{+}/Ca^{2+} exchanger. Am J Physiol Cell Physiol. 2004; 287:C1167–C1172. [PubMed: 15475515]

Husain M, Jiang LW, See V, Bein K, Simons M, Alper SL, Rosenberg RD. Regulation of vascular smooth muscle cell proliferation by plasma membrane Ca2+-ATPase. Am J Physiol Cell Physiol. 1997; 41:C1947–C1959.

James P, Vorherr T, Krebs J, Morelli A, Castello G, McCormick DJ, Penniston JT, De Flora A, Carafoli E. Modulation of erythrocyte Ca^{2+}-ATPase by selective calpain cleavage of the calmodulin-binding domain. J Biol Chem. 1989; 264:8289–8296. [PubMed: 2542272]

Kip SN, Gray NW, Burette A, Canbay A, Weinberg RJ, Strehler EE. Changes in the expression of plasma membrane calcium extrusion systems during the maturation of hippocampal neurons. Hippocampus. 2006; 16:20–34. [PubMed: 16200642]

Martin LJ, Al-Abdulla NA, Brambrink AM, Kirsch JR, Sieber FE, Portera-Cailliau C. Neurodegeneration in excitotoxicity, global cerebral ischemia, and target deprivation: a perspective on the contributions of apoptosis and necrosis. Brain Res Bull. 1998; 46:281–309. [PubMed: 9671259]

Nicholls DG. Mitochondrial dysfunction and glutamate excitotoxicity studied in primary neuronal cultures. Curr Mol Med. 2004; 4:149–177. [PubMed: 15032711]

Paszty K, Verma AK, Padanyi R, Filoteo AG, Penniston JT, Enyedi A. Plasma membrane Ca2+ ATPase isoform 4b is cleaved and activated by caspase-3 during the early phase of apoptosis. J Biol Chem. 2002; 277:6822–6829. [PubMed: 11751908]

Paszty K, Antalffy G, Penheiter AR, Homolya L, Padanyi R, Ilias A, Filoteo AG, Penniston JT, Enyedi A. The ca-spase-3 cleavage product of the plasma membrane Ca(2+)-ATPase 4b is activated and appropriately targeted. Biochem J. 2005; 391:687–692. [PubMed: 16080782]

Piser TM, Lampe RA, Keith RA, Thayer SA. w-Grammotoxin blocks action-potential-induced Ca^{2+} influx and whole-cell Ca^{2+} current in rat dorsal root ganglion neurons. Pfluger's Arch Eur J Physiol. 1994; 426:214–220. [PubMed: 8183632]

Pottorf WJ, Thayer SA. Transient rise in intracellular calcium produces a long-lasting increase in plasma membrane calcium pump activity in rat sensory neurons. J Neurochem. 2002; 83:1002–1008. [PubMed: 12421373]

Randall RD, Thayer SA. Glutamate-induced calcium transient triggers delayed calcium overload and neurotoxicity in rat hippocampal neurons. J Neurosci. 1992; 12:1882–1895. [PubMed: 1349638]

Sato K, Saito Y, Kawashima S. Identification and characterization of membrane-bound calpains in clathrin-coated vesicles from bovine brain. Eur J Biochem. 1995; 230:25–31. [PubMed: 7601107]

Sattler R, Tymianski M. Molecular mechanisms of glutamate receptor-mediated excitotoxic neuronal cell death. Mol Neurobiol. 2001; 24:107–129. [PubMed: 11831548]

Schwab BL, Guerini D, Didszun C, et al. Cleavage of plasma membrane calcium pumps by caspases: a link between apoptosis and necrosis. Cell Death Differ. 2002; 9:818–831. [PubMed: 12107825]

Schwiening CJ, Kennedy HJ, Thomas RC. Calcium hydrogen exchange by the plasma membrane Ca-ATPase of voltage-clamped snail neurons. Proc R Soc Lond. 1993; 253:285–289.

Thayer SA, Sturek M, Miller RJ. Measurement of neuronal Ca^{2+} transients using simultaneous microfluorimetry and electrophysiology. Pfluger's Arch Eur J Pharmacol. 1988; 412:216–223. [PubMed: 3174384]

Thayer SA, Usachev YM, Pottorf WJ. Modulating Ca^{2+} clearance from neurons. Front Biosci. 2002; 7:D1255–D1279. [PubMed: 11991858]

Tymianski M, Charlton MP, Carlen PL, Tator CH. Secondary Ca-2+ overload indicates early neuronal injury which precedes staining with viability indicators. Brain Res. 1993; 607:319–323. [PubMed: 7683241]

Usachev YM, DeMarco SJ, Campbell C, Strehler EE, Thayer SA. Bradykinin and ATP accelerate Ca^{2+} efflux from rat sensory neurons via protein kinase C and the plasma membrane Ca^{2+} pump isoform 4. Neuron. 2002; 33:113–122. [PubMed: 11779484]

Wang GJ, Randall RD, Thayer SA. Glutamate-induced intracellular acidification of cultured hippocampal neurons demonstrates altered energy metabolism resulting from Ca^{2+} loads. J Neurophysiol. 1994; 72:2563–2569. [PubMed: 7897473]

Werth JL, Thayer SA. Mitochondria buffer physiological calcium loads in cultured rat dorsal root ganglion neurons. J Neurosci. 1994; 14:348–356. [PubMed: 8283242]

Werth JL, Usachev YM, Thayer SA. Modulation of calcium efflux from cultured rat dorsal root ganglion neurons. J Neurosci. 1996; 16:1008–1015. [PubMed: 8558228]

Wu HY, Yuen EY, Lu YF, Matsushita M, Matsui H, Yan Z, Tomizawa K. Regulation of *N*-methyl-D-aspartate receptors by calpain in cortical neurons. J Biol Chem. 2005; 280:21 588–21 593.

Xia ZG, Dudek H, Miranti CK, Greenberg ME. Calcium influx via the NMDA receptor induces immediate early gene transcription by a MAP kinase/ERK-dependent mechanism. J Neurosci. 1996; 16:5425–5436. [PubMed: 8757255]

Xing H, Azimi-Zonooz A, Shuttleworth CW, Connor JA. Caffeine releasable stores of Ca2+ show depletion prior to the final steps in delayed CA1 neuronal death. J Neurophysiol. 2004; 92:2960–2967. [PubMed: 15201305]

Yoon WJ, Won SJ, Ryu BR, Gwag BJ. Blockade of ionotropic glutamate receptors produces neuronal apoptosis through the Bax-cytochrome C-caspase pathway: the causative role of Ca2+ deficiency. J Neurochem. 2003; 85:525–533. [PubMed: 12675929]

Zaidi A, Barron L, Sharov VS, Schoneich C, Michaelis EK, Michaelis ML. Oxidative inactivation of purified plasma membrane Ca2+-ATPase by hydrogen peroxide and protection by calmodulin. Biochemistry. 2003; 42:12 001–12 010.

Zenisek D, Matthews G. The role of mitochondria in presynaptic calcium handling at a ribbon synapse. Neuron. 2000; 25:229–237. [PubMed: 10707986]

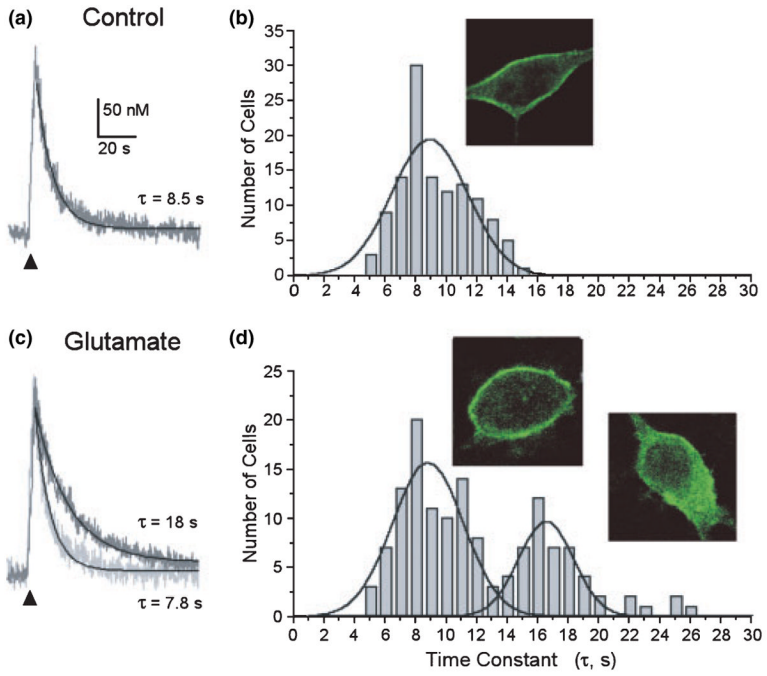

Fig. 1.

Slowed $[Ca^{2+}]_i$ clearance in a population of glutamate-treated hippocampal neurons. (a) Representative $[Ca^{2+}]_i$ recording from a single hippocampal neuron in the presence of 5 μM CPA and 10 μM CNQX. $[Ca^{2+}]_i$ was measured with indo-1-based photometry, as described in Methods. Trains of action potentials were elicited by electric-field stimulation (8 Hz, 4 s) to produce a small increase in $[Ca^{2+}]_i$. The recovery phase of the $[Ca^{2+}]_i$ response was fit with a single exponential equation as described in Methods (solid line) to determine the time constant for recovery shown (τ). (b) Frequency histogram displays the number of cells with the indicated time constant for recovery (τ-values were binned over 1 s). Inset shows a confocal image of a single hippocampal neuron labeled with pan-anti-PMCA antibody 5F10. Immunocytochemistry was performed as described in Methods. (c) $[Ca^{2+}]_i$ recorded as in (a) but 4 h after a 30 min exposure to 200 μM glutamate. Recordings from two representative cells are superimposed. (d) Frequency histogram from glutamate-treated cells was fit with two Gaussian curves (solid lines) as described in Methods. Insets: confocal imaging of cells labeled with pan-anti-PMCA antibody 5F10 4 h after glutamate treatment showed two populations of cells, those with predominantly plasma membrane localized fluorescence and cells with internalized fluorescence.

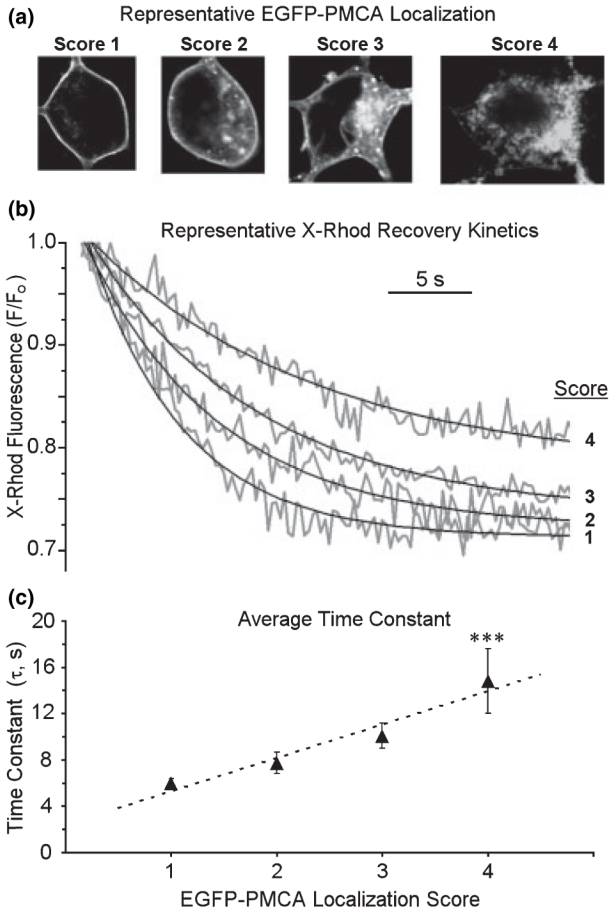

Fig. 2.

Loss of plasma membrane localized PMCA predicts impaired Ca^{2+} clearance. Confocal imaging of hippocampal neurons was performed 4 h after a 30 min treatment with 200 μM glutamate. (a) Representative confocal images of cells expressing EGFP-PMCA4b were scored as indicated. (b) After scoring, single cell $[Ca^{2+}]_i$ recovery kinetics were measured using X-rhod-based confocal imaging as described in Methods. Representative traces show recovery phases from cells with the scores indicated. (c) The graph summarizes pooled data from experiments such as those shown in (b). Each data point is the mean ± SEM of 6–20 recordings; ***$p < 0.001$, significantly different from scores 1–3 determined by two-way ANOVA with Fisher's PLSD posthoc test. The X-rhod-1 fluorescence intensities were not converted to $[Ca^{2+}]_i$ because of potential inaccuracies associated with calibrating a single wavelength Ca^{2+} indicator. Thus, τ-values from confocal imaging are not directly comparable with those obtained from photometry experiments described in Fig. 1, in which the ratiometric indicator indo-1 was used and the data were fully calibrated.

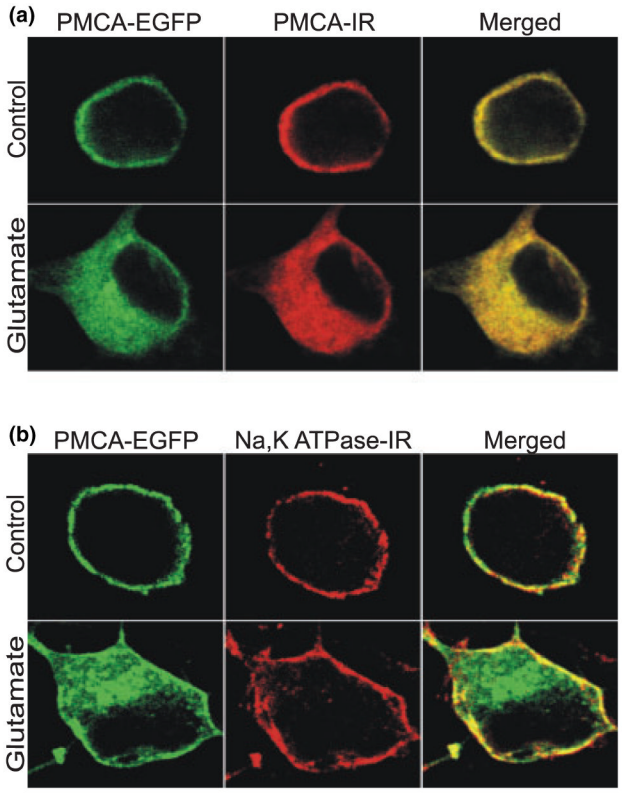

Fig. 3.

Selective internalization of the PMCA. At 48 h after transfection with EGFP-PMCA4b, hippocampal cultures were treated as described, then fixed and labeled with antibody to either hPMCA4 (a) or antibody to the α5 subunit of the Na^+/K^+ ATPase (b). In the representative confocal images, EGFP is shown in green; hPMCA4 (PMCA-IR) and Na^+/K^+ ATPase (Na, K ATPase-IR) immunoreactivity are shown in red; and overlap in the merged images is indicated by yellow. Upper row shows images from an untreated cell (control) and bottom row shows a cell 4 h after a 30 min treatment with 200 μM glutamate. Images are representative of 20 PMCA-IR and 45 Na, K ATPase-IR cells.

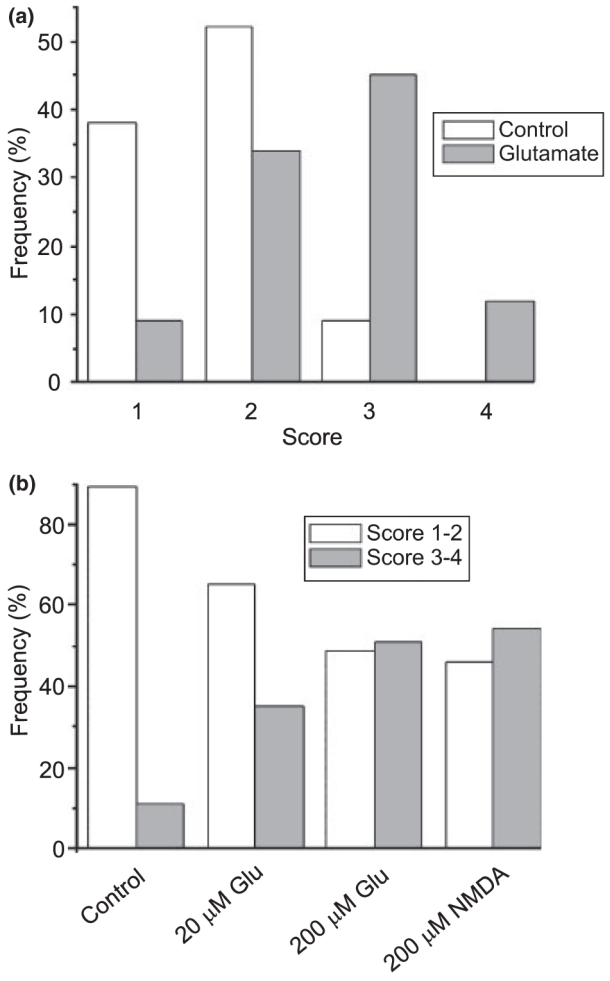

Fig. 4.

Glutamate induces internalization of EGFP-PMCA following activation of NMDA receptors. (a) EGFP-PMCA4b-expressing cells were sham-treated (control, open bars) or treated with 200 μM glutamate for 30 min (glutamate, solid bars). At 4 h after starting treatment with agonist, cells were imaged by confocal microscopy. Images were scored using the system described in Fig. 2 (1 = plasma membrane localized; 4 = internalized) by an investigator uninformed of the treatment. (b) EGFP-PMCA4b-expressing cells were sham-treated (control), treated with 20 μM glutamate for 30 min (20 μM Glu), treated with 200 μM glutamate for 30 min (200 μM Glu) or treated with 200 μM NMDA for 30 min (200 μM NMDA). At 4 h after starting treatment with agonist, cells were imaged by confocal microscopy. Images were scored using the system described in Fig. 2 (1 = plasma membrane localized; 4 = internalized) by an investigator uninformed of the treatment. Bar graph displays the frequency of cells scored 1–2 (open bars) and the frequency of cells scored 3–4 (solid bars) from 130 control cells, 35 cells treated with 20 μM glutamate, 124 cells treated with 200 μM glutamate and 35 NMDA-treated cells.

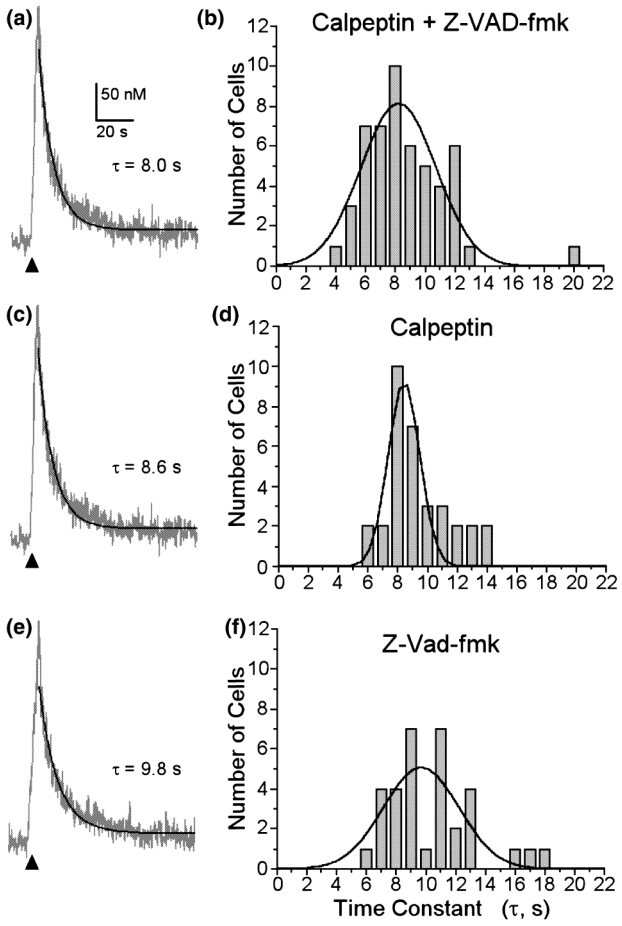

Fig. 5.

Protease inhibitors protect hippocampal neurons from glutamate-induced slowing of Ca^{2+} efflux. At 60 min prior to glutamate treatment (30 min, 200 μM), hippocampal cultures were treated with 10 μM calpeptin and 100 μM Z-VAD-fmk in combination (a and b), calpeptin alone (c and d) or Z-VAD-fmk alone (e and f). The cells were maintained in protease inhibitors throughout the experiment. (a), (c) and (e) Representative $[Ca^{2+}]_i$ recordings from single hippocampal neurons in the presence of 5 μM CPA and 10 μM CNQX. $[Ca^{2+}]_i$ was recorded 4 h after glutamate treatment with indo-1-based photometry as described in Methods. Trains of action potentials were elicited by electric-field stimulation (8 Hz, 4 s) to produce a small increase in $[Ca^{2+}]_i$ (150–400 nM). The recovery phase of the $[Ca^{2+}]_i$ response was fit with a single exponential equation as described in Methods (solid line) and the time constant for recovery shown (τ). (b), (d) and (f) Frequency histograms from cells receiving the indicated protease inhibitors prior to treatment with glutamate.

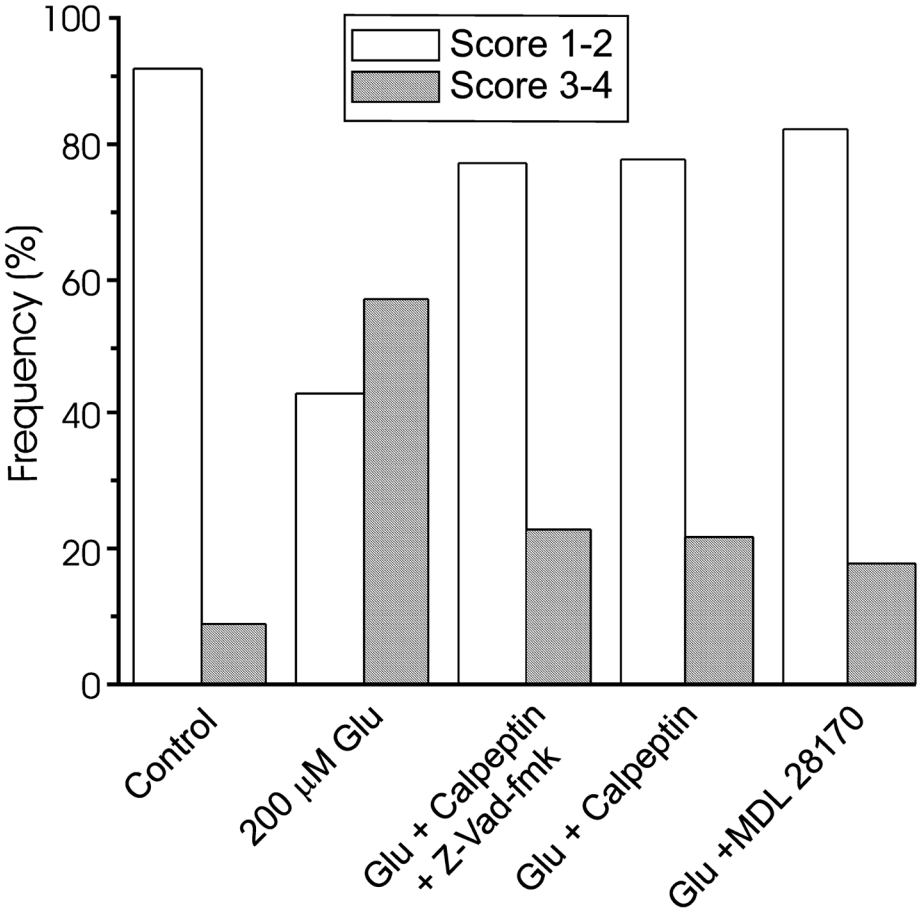

Fig. 6.

Protease inhibitors prevent glutamate-induced internalization of EGFP-PMCA. EGFP-PMCA4b-expressing cells were treated as indicated: sham (control), 200 μM glutamate for 30 min (200 μM Glu), incubated for 60 min with 10 μM calpeptin and 100 μM Z-VAD-fmk in combination followed by 30 min treatment with glutamate (Glu + calpeptin + Z-VAD), 60 min with 10 μM calpeptin followed by 30 min treatment with 200 μM glutamate (Glu + calpeptin), 60 min with 10 μM MDL 28170 followed by 30 min treatment with 200 μM glutamate (Glu + MDL 28170). For the experiments with protease inhibitors, the inhibitors remained in the medium throughout the 4 h experiment. At 4 h after starting the glutamate treatment, cells were imaged by confocal microscopy. Images were scored using the system described in Fig. 2 (1 = plasma membrane localized; 4 = internalized) by an investigator uninformed of the treatment. Data for control and glutamate-treated cells were re-plotted from Fig. 4 for comparison purposes. Bar graph displays the frequencies of binned scores of 1–2 (open bars) and 3–4 (solid bars) from 130 control cells, 124 glutamate-treated cells, 60 glutamate + calpeptin + Z-VAD-fmk-treated cells, 32 glutamate + calpeptin-treated cells and 17 glutamate + MDL 28170-treated cells.

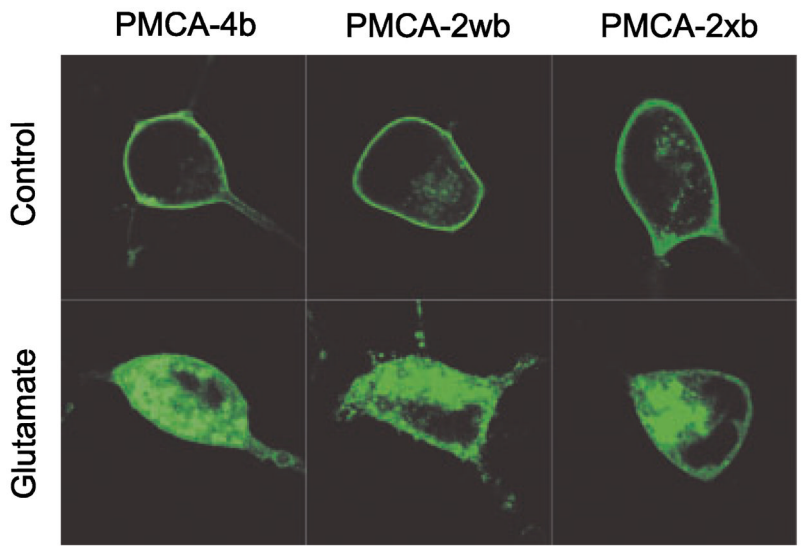

Fig. 7.

Glutamate-induced PMCA internalization is not isoform specific. Representative confocal images from neurons expressing EGFP-PMCA4b (left column), EGFP-PMCA2wb (middle column) and EGFP-PMCA2xb (right column) are shown from untreated cultures (upper row) and cultures 4 h after a 30 min treatment with 200 μM glutamate (bottom row). Confocal imaging and transfection were performed as described in Methods.